Final Progress Report

As summarized below, we have made significant progress towards achieving the goals of our project. *We demonstrated monolithic integration of CMUT arrays with CMOS front-end electronics, and designed, fabricated and tested novel mass loaded, dual-electrode CMUTs with high coupling coefficient and bandwidth. In addition to these significant achievements which make CMUTs more viable for IVUS applications, we performed initial imaging experiments with annular arrays operating around 50MHz showing the expected clear advantages of dynamic receive focusing.*

Studies and Results

Aim 1. Fabricate broadband CMUT arrays with integrated electronics for IVUS catheters

In order to implement a low-cost, high performance silicon based IVUS imaging device, integration of optimized front-end electronics and CMUT transducer array elements on a single chip is critical. As depicted schematically in **Figure 1**, this approach a) eliminates the parasitic capacitance due to interconnect between the electronics and CMUT array element, critical for achieving high SNR from small CMUT elements, b) overcomes the chip-to-chip electrical interconnect problem that requires flip-chip bonding and through wafer vias, complex manufacturing steps reducing the yield and signal quality due to considerable wire bond pad capacitance.

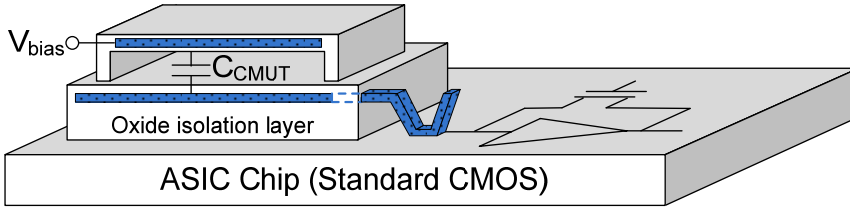

Figure 1. Schematic of the monolithic CMUT-on-CMOS integration concept.

Recently, we demonstrated monolithic integration of CMUT and CMOS electronics. This was based on a wafer scale CMOS electronics fabrication run with a commercial entity using 0.35u, 3.3V TSMC process. We essentially re-designed the electronics used for wire bonded testing for this technology. In addition, the transmitters, logic circuitry and cable drivers were designed with layout compatible with the CMUT imaging arrays, since the electrodes of the capacitive array elements need to be connected directly to the inputs of the array of matching amplifiers. The completion of this wafer run was a significant milestone for our CMUT-on-CMOS research.

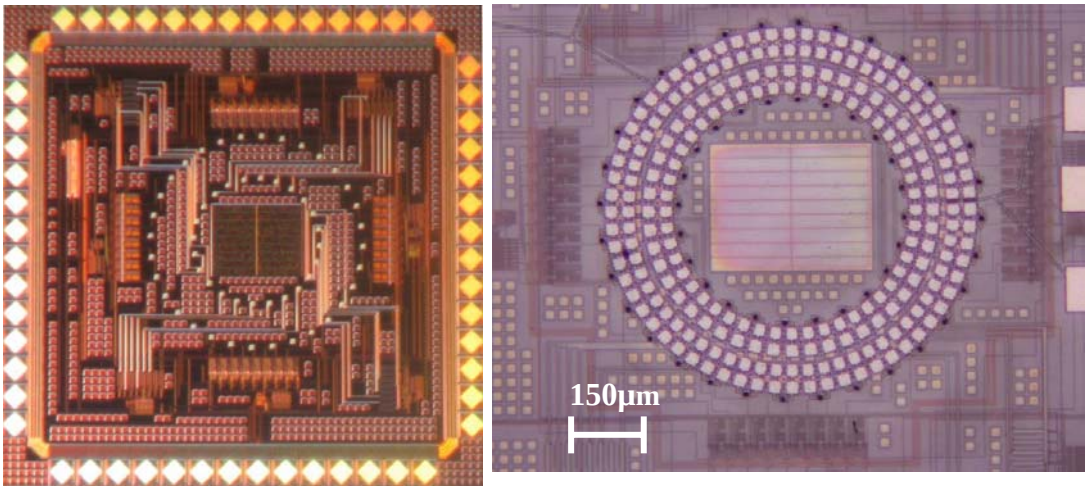

Figure 2. Left: CMOS electronics chip with electronics for 32Rx-24Tx dual-ring CMUT array. Right: The same chip after CMUT-on-CMOS fabrication.

CMUT arrays were fabricated on the CMOS electronics and initial tests were performed. **Figure 2** shows micrographs of one set of CMOS electronics for dual-ring arrays before CMUT fabrication on the left. The figure also shows the same circuit after a dual-ring array was fabricated on top of the same electronics. As seen in the picture, the top electrodes of the CMUTs are directly connected to the inputs of the underlying electronics, reducing the parasitic capacitance and achieving the single chip CMUT array with electronics structure. As the final test of feasibility demonstration, the chips were coated with parylene and immersed in water tank where a single Tx-Rx pair on a CMUT-on-CMOS dual-ring array with integrated electronics was used to transmit and receive ultrasonic waves. **Figure 3** shows the pulse echo signal from water-air interface 3.6mm away from the CMUT-on-CMOS chip amplified and multiplexed by the on chip electronics. The single shot SNR is over 40dB for this signal, which has 87% -

6dB FBW around center frequency of 16.7MHz, mainly limited by silicon substrate ringing and cross-talk effects.

High-voltage pulser designs

We also designed and tested high voltage transmitters separately on the same CMOS run. We used using special layout techniques to overcome the 3.3V supply limitation and generate high voltage pulses to drive CMUTs. **Figure 4** shows a measurement on a pulser where we were able to obtain peak pulse voltages up to 35V with a control 3.3V control signal. *These results indicate that we are able to design and fabricate low noise TIAs and high voltage pulsers on the same standard CMOS wafer from commercial foundry for single-chip CMUT imaging arrays using CMUT-on-CMOS technology.* This is a clear demonstration of CMUT-on-CMOS technology, Specific Aim 1 of the project.

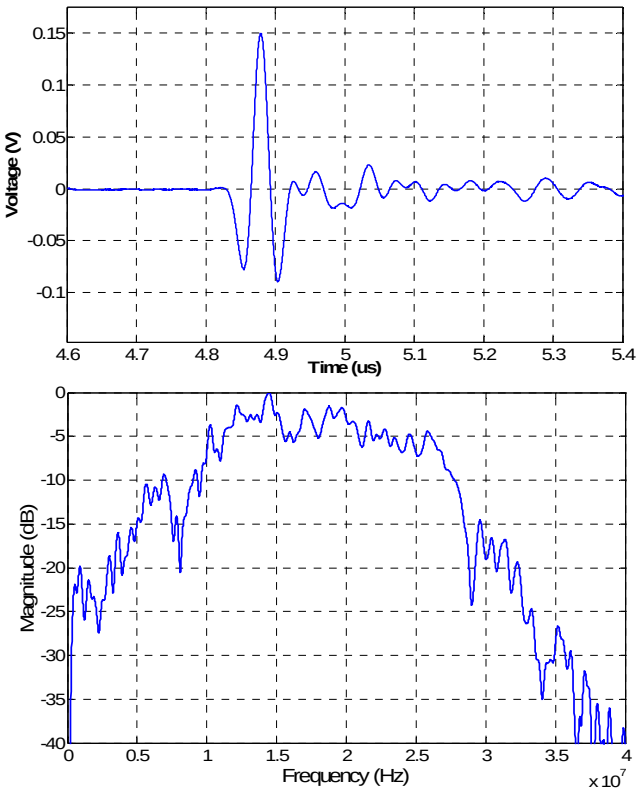

Figure 3. Top: The pulse-echo signal obtained from a dual-ring array made by CMUT-on-CMOS technology. Bottom: The frequency spectrum of the signal.

Aim 2. Development dual electrode and mass loaded CMUTs for high performance, high bandwidth operation

A major perceived weakness of the CMUT technology has been the low overall sensitivity, which offset its broad bandwidth advantage. We developed the dual-electrode (D-E) CMUTs to improve the overall performance of the CMUTs by effectively implementing a separately optimized transmitter and a receiver using the same CMUT membrane. During the course of our current project, we demonstrated pulse-echo or monostatic operation of the DE-CMUT, where the bias on the membrane should be changed dynamically during a single transmit-receive cycle. This approach, which used a uniform CMUT membrane, showed an overall improvement of 16.4dB (9dB in receive sensitivity, and 7.4dB in transmit pressure). The maximum peak pressure output for a 10MHz element with a tone burst drive was 1.6MPa, a significant value that may be useful for therapeutic applications. Although this improvement was significant, the bandwidth of the DE-CMUT was not improved as compared to the conventional CMUT.

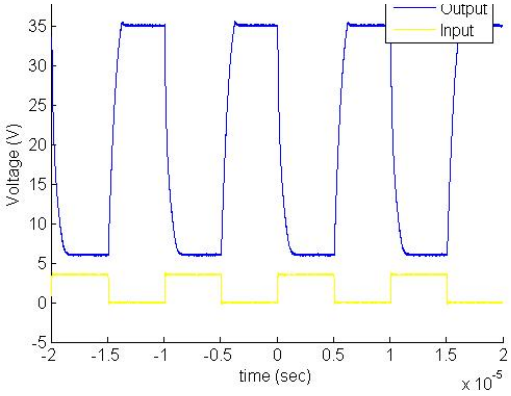

Figure 4. Measured output of a HV pulser (upper curve) when driven by a 5MHz, 3.3V square wave. The output pulse has a 25V peak swing that can be improved to 35V to drive a CMUT.

We had performed a detailed investigation into the design space of CMUTs with non-uniform membrane DE-CMUTs to find out optimized structures for advanced applications like harmonic imaging. Using finite element analysis based simulations we compared conventional and DE-CMUTs with uniform and non-uniform membranes. We used the electromechanical coupling coefficient, k^2, as a metric to help compare the CMUTs to piezoelectric transducers, in addition to calculating bandwidth and transmit sensitivity in Pa/V. The analysis on uniform membranes showed the sensitivity-bandwidth tradeoff for this structure. *The conclusion is that one cannot obtain both high bandwidth and high coupling with a conventional CMUT with a single electrode, verifying the observations. More importantly, our analysis of mass-loaded DE-CMUTs showed that this structure solves this dilemma.*

The summary of results of this analysis is shown in Table 2. **The results are striking: With a mass-loaded DE-CMUT structure, one can obtain both high bandwidth (140% FBW) and high coupling coefficient, k^2~0.85. This figure is equal or better than the best single crystal piezoelectrics and the bandwidth is suitable for harmonic imaging.**

Table 2. Membrane geometry and corresponding operation parameters for conventional CMUT and DE-CMUT with uniform and non-uniform membrane.

	Center/ Side Collapse Voltage (V)	Coupling Coef. (k^2) (90% V_{col})	Fractional Bandwidth (%)	Pressure Output (MPa)	Transmit Sensitivity (KPa/V)
Conventional CMUT	115/NA	0.24	80	0.66	12.1
Dual-elect. CMUT	76/160	0.71	80	1.48	12.3
Dual-elec. CMUT with center mass	74/132	0.85	140	1.53	15.4

This is achieved with a small increase in the DC bias level (Row 3 in Table 2) as compared to a conventional CMUT. More importantly, this performance is achieved when the device is biased 90% of its collapse voltage (Vcol). To test our predictions, we fabricated mass-loaded DE-CMUTs as well as other types for comparison. **Figure 5** shows a scanning electron micrograph of a typical mass-loaded DE-CMUT with 2.75µm thick membrane with a 1.5µm thick, 10 µm wide center section. **Figure 6** shows calculated (A) and measured (B) coupling coefficient, k^2, as a function of DC bias normalized to the collapse voltage for different CMUT designs. For a conventional CMUT with uniform membrane, k^2 reaches 0.8 only at 98-99% of Vcol, whereas the mass-loaded DE-CMUT attains that value at 88% of Vcol. As shown in Fig. 14, measured and predicted k^2 values agree very well, for example we measured k^2 =0.82 at 90% of Vcol for a prediction of 0.85. *This has a practical significance, showing that one has a much wider DC operation range for efficient operation for a mass-loaded DE-CMUT, making it immune to array non-uniformities and non ideal behavior such as charging.*

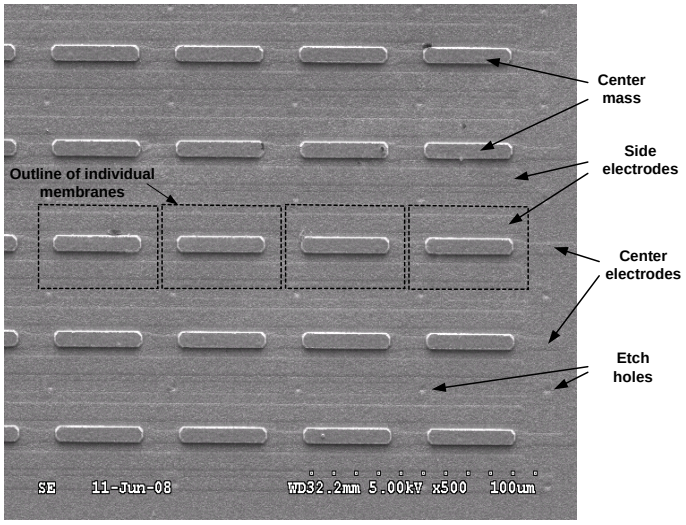

Figure 5. SEM of a fabricated mass loaded DE-CMUT with rectangular membranes.

We also measured the bandwidth of these transducers by performing transmission experiments using a hydrophone in a water tank. The result of this measurement is shown in **Figure 7** along with model predictions for DE-CMUTs with uniform and non-uniform membrane. The results indicate that the same DE-CMUT has 134% FBW as compared to 80% FBW as well as ~3dB improvement in transmit sensitivity as compared to the uniform membrane DE-CMUT. Overall, the performance improvement over conventional CMUT is about 20dB for this particular case. We note that these coupling figures are given for the center electrode while the side electrodes are kept at a constant bias. Therefore, one can achieve significant sensitivity

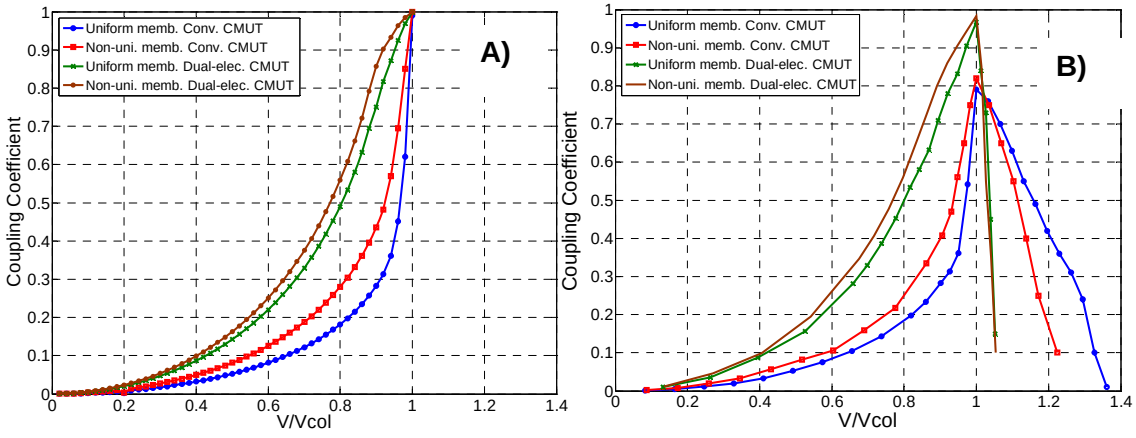

Figure 6. A) Calculated B) measured variation of coupling coefficient as a function of normalized DC bias.

improvement as well as broad bandwidth without increasing system complexity with mass-loaded DE-CMUT. **These results show significant progress in Specific Aim 2 of the current project.**

Finally, to see the effect of these improvements in a realistic scenario, we imaged a 4 wire target in oil by scanning a conventional CMUT and a mass-loaded DE-CMUT in the same array with the same input pulse and DC bias set at 90% of Vcol of each device. The resulting images are shown in Figure 8. With its higher sensitivity and pressure output, the DE-CMUT is able to image deeper and resolve all targets with 30dB dynamic range, whereas the conventional CMUT fails to image the 4th wire even with 20dB dynamic range. **Therefore, having verified our models, we expect a significant improvement in IVUS imaging when we implement annular arrays using this new type of CMUT transducer developed as part of our current project.**

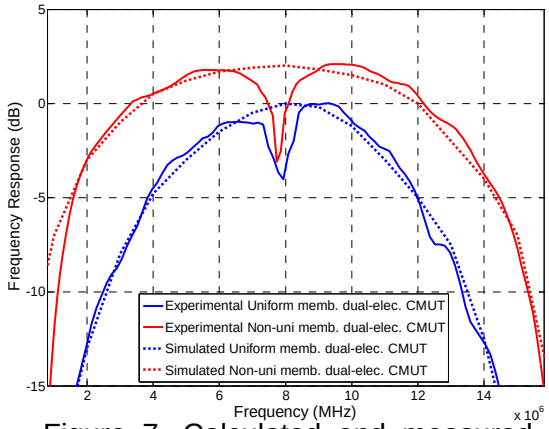

Figure 7. Calculated and measured spectra for DE-CMUTs with uniform and non-uniform membranes.

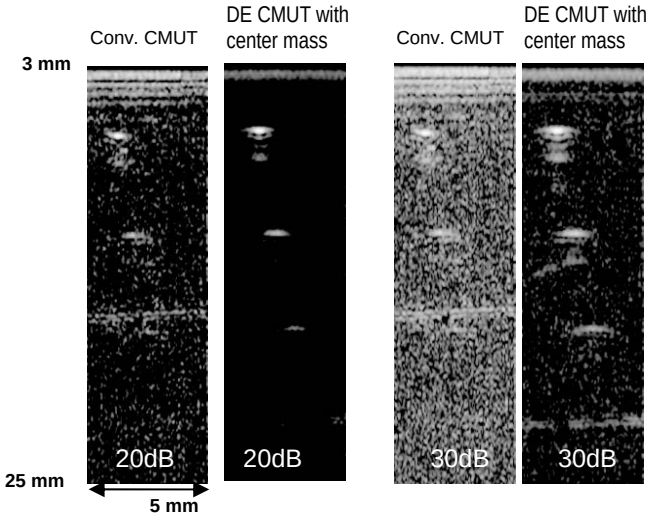

Figure 8. Wire target images obtained by conventional and mass-loaded DE-CMUTs with the same witdh and designed to operate at the same frequency. DE-CMUT improves the penetration depth.

<u>Imaging experiments with 50MHz, dynamic focusing CMUT annular arrays for IVUS</u>

Current IVUS arrays operate up to 40MHz and with 20-30% fractional bandwidth and use a single, focused transducer element. As part of our project, we fabricated CMUT annular array with 50MHz center frequency. This array has a center frequency higher than the commercial single element IVUS probes that are used today, and it provides dynamic focusing capability due to its array structure. To operate this array in water, we used a 3µm thick parylene coating, an inert and biocompatible polymer which provides electrical isolation but does not affect the CMUT dynamics. In the imaging experiments, 25µm diameter wire targets are located at 1.6 mm, (f# of 1.9) 2.4 mm (f# of 2.9) and 3.2 mm (f# of 3.8) away from the array. A linear scan is performed using a linear actuator to move the phantom across the array for 2.25 mm with 150 steps while the RF data set from 7 transmit-receive pairs is collected at each step. Each echo signal was filtered using a bandpass filter with a pass band of 25-65 MHz. The ranges of signal and SNR data are 4 mV - 13 mV and 12 dB - 22 dB. These variations are mostly due to the differences in element sizes and diffraction loss among the array elements.

Image reconstruction in linear-scan format was performed using synthetic aperture processing with three different focusing schemes. Each image line was reconstructed by through synthetic beamforming using echo signals acquired from 7-transmit-receive element pairs. The resulting images are shown in **Figure 9-A** with 20 and 40 dB dynamic range. The image depth extends from 1.36 mm to 3.55 mm (f/1.6 to (f/4.2). **Figure 9-B** shows the 1-D Lateral cross-sections along the 3rd target. The fixed focusing is located at the second target. These images reflect the first demonstration of the resolution and penetration capability of a 50-MHz CMUT annular array. The 6-dB lateral and axial point resolutions measured on the 3rd target (at f/3.8) approximately 120 µm, and 35 µm, respectively. These resolutions are consistent with theoretical expectations for an annular array with identical parameters (the lateral and axial resolutions are approximately 105 µm and 37 µm, respectively). These values are suitable for measuring the thickness of vulnerable plaques, an important metric for a high frequency IVUS probe. The unexpected asymmetry in lateral response should be due to the aperture non-uniformity. Comparison of the three columns indicate that fixed focusing, as expected, increases the side-lobe levels and image noise floor. **In other words, a considerable improvement in image quality is demonstrated by using dynamic receive focusing with this annular array, even the reconstruction was**

based on synthetic aperture processing. Figure 9-C shows the beamformed echo signal and its spectrum associated with the 3rd target. This spectrum represents the overall frequency response of the array, and shows approximately a 6-dB FBW of 37% around 53 MHz, and 12-dB FBW of 58% around 50 MHz. The spectrum has not been corrected for diffraction and the attenuation in water. *The device bandwidth is mainly limited by the cross-talk in the array which causes the dips at 30MHz and 65MHz, which was verified by our finite element modeling.*

Publications

Peer-Reviewed Journal Papers

1. R.O. Guldiken, M. Balantekin, J. Zahorian, and F. L. Degertekin, "Characterization of Dual-Electrode CMUTs: Demonstration of Improved Receive Performance and Pulse Echo Operation with Dynamic Membrane Shaping," IEEE Trans. on UFFC, **55**, pp. 2236-45, 2008.
2. R.O. Guldiken, J. Zahorian, F.Y. Yamaner, and F. L. Degertekin, "Dual Electrode CMUTs with Non-uniform Membranes for High Electromechanical Coupling Coefficient and High Bandwidth Operation," IEEE Trans. on UFFC, **56**, pp. 1270-6, 2009.

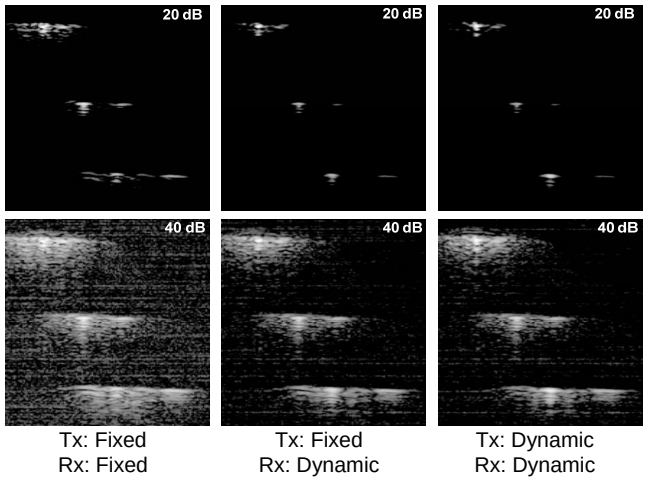

A)

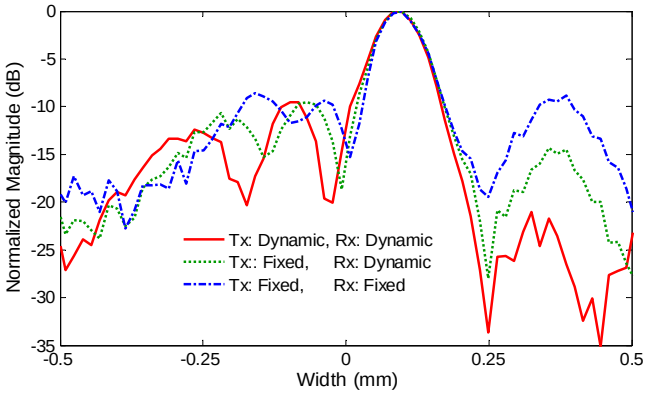

B)

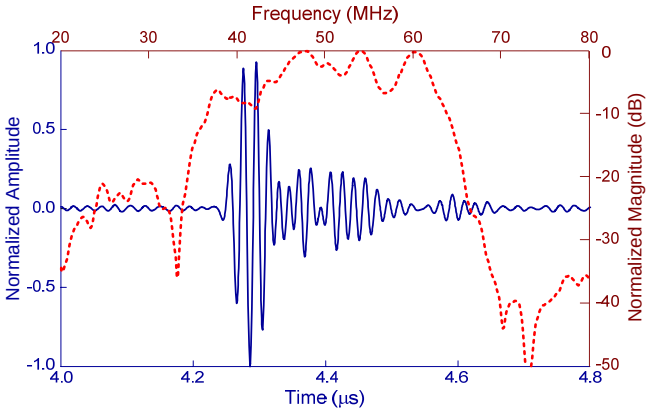

C)

Figure 9 A) Linear-scan images of 3 wire targets. Fixed focus is located at a depth of the 2nd target. The image depth (top to bottom) extends from 1.36 mm to 3.55 mm (f/1.6 to (f/4.2), and the image width is 2.25 mm. The 6-dB lateral and axial point resolutions measured on the 3rd target (at f/3.8) are approximately 120 μm, and 35 μm, respectively. Top row 20dB, bottom row 40dB dynamic range B) 1-D Lateral cross-sections along the 3rd target. C) The axial response measured on the 3rd target showing a 6-dB FBW of 37% around 50 MHz, and 10-dB FBW of 40% FBW at 53 MHz.